The Journal of Experimental Biology **198**, 2115–2125 (1995)
Printed in Great Britain © The Company of Biologists Limited 1995

ELECTROPHYSIOLOGY OF K^+ TRANSPORT BY MIDGUT EPITHELIUM OF LEPIDOPTERAN INSECT LARVAE

IV. A MULTICOMPARTMENT MODEL ACCOUNTS FOR TETRAMETHYLAMMONIUM ENTRY INTO GOBLET CAVITIES

ALAN KOCH AND DAVID F. MOFFETT

Laboratory of Molecular Physiology, Zoophysiology Program, Washington State University, Pullman, WA 99164-4326, USA

Accepted 19 June 1995

Summary

A quantitative model was developed to explain the kinetics of tetramethylammonium (TMA^+) movement into and out of the goblet cavities of posterior midgut cells of *Manduca sexta* based on the data of the accompanying paper, which indicated that TMA^+ does not enter the goblet cavity directly from the lumen.

The model has two cellular compartments between the lumen and goblet cavity; these have been tentatively identified as the columnar cell and goblet cell cytoplasm. Five transmembrane pathways are included: from lumen to columnar cell, from columnar cell to goblet cell, from goblet cell cytoplasm to goblet cell cavity, and across the basal membrane of each cell type. These pathways need not be channels; they could use endocytotic or exocytotic mechanisms or, in the case of the cell-to-cell passage, septate junctions. However, in all cases, transfer is proportional to the electrochemical gradient.

The model was tested against the results obtained after exposure to TMA^+ in short-circuited and open-circuited tissues as well as results from an open-circuited tissue that did not develop a large transepithelial potential. Although driving forces for TMA^+ across the membrane barriers were quite different in the different experimental conditions, the transfer coefficients from lumen to columnar cell, from columnar to goblet cell and from both cells across the basal membrane were the same. The only transfer coefficient that changed between short-circuit and open-circuit conditions was that from goblet cell cytoplasm to goblet cavity. This value was high under short-circuit conditions (when K^+ transport activity is high), but low under open-circuit conditions (when K^+ transport activity is low).

The model suggests a hypothesis in which TMA^+ enters the goblet cavity by an indirect route across the cell membrane of columnar cells, and thence passes to the goblet cell cytoplasm through intercellular junctions. Results from experiments with cytochalasin E suggest that the actin-based cytoskeleton is involved in limiting cell–cell coupling. In this model, TMA^+ passes from the goblet cell cytoplasm to the goblet cavity *via* the K^+/nH^+ antiport believed to mediate active transepithelial K^+ transport. However, although actively transported K^+ is believed to pass from goblet cavity to lumen, TMA^+ cannot.

Key words: insect, midgut, active K^+ transport, goblet cells, compartmental model, *Manduca sexta*.

Introduction

Considerable evidence suggests that the goblet cells of lepidopteran larval midgut are responsible for the high rate of active K^+ transport across the epithelium from the hemolymph side to the lumen as measured in isolated midgut preparations (Dow, 1986; Harvey, 1992). Goblet cells are characterized by an apical cavity separated from the gut lumen by a valve-like structure. The currently accepted model of K^+ transport (Harvey, 1992; Zeiske, 1992) places an active step at the goblet cell apical membrane (GCAM). This model requires a net efflux of K^+ from the cavity to the lumen, which has been assumed to occur by passive diffusion through the valve.

Moffett *et al.* (1995) presented evidence that tetramethylammonium (TMA^+), applied to the luminal side of the isolated midgut as a tracer for free diffusional movement of small cations, does not have ready access to the goblet cavities. In more than half of the cavities, no entry of TMA^+ could be measured. In the remaining cavities, the slow uptake rates and the higher-order kinetics of the influx and efflux curves of TMA^+ suggested that TMA^+ enters and leaves the cavities by an indirect route. This paper formally analyzes the influx and efflux curves for evidence of multicompartment kinetics and presents a model that rationalizes the distribution of TMA^+ in the tissue.

Materials and methods

Experimental

Methods for obtaining TMA^+ influx and efflux curves were described in Moffett *et al.* (1995). Briefly, measurement of $[TMA^+]$ in goblet cavities and cytoplasm rests on the fact that the K^+-selective ion-exchange resin used in microelectrodes has a very high selectivity for quaternary amines over K^+. As in previous studies in this series (Moffett and Koch, 1988*a*,*b*), we used double-barreled intracellular microelectrodes in which one barrel contains K^+-selective resin and the other serves as a reference. In such electrodes, the difference between the output of the two barrels is a measure of the ionic activity. For K^+ calibration, the relationship between concentration and activity was determined from standard tables and the values given are in activity units. For TMA^+ there are no published values, so the values given here are in concentration units assuming that activity equals concentration.

The stable difference trace after an impalement had been established, and before administration of TMA^+, was taken as a measure of K^+ activity. After TMA^+ superfusion of the luminal side of the gut had been started, the change in voltage difference between the electrode barrels was taken as a measure of TMA^+ activity. Typically, the difference trace was sampled every 20 s, although sampling intervals ranged from 10 to 50 s as appropriate in some experiments. For each sample, the concentration of TMA^+ (indicated as $[TMA^+]_c$ for cytoplasm or $[TMA^+]_g$ for goblet cavities) was calculated from the TMA^+ calibration of the electrode pair. Derivatives of each data set were formed by central difference. The set of derivatives was filtered using a moving average with a window of three. Phase plane diagrams were constructed from the values of $[TMA^+]$ and the filtered values of $d[TMA^+]/dt$.

Analysis

If TMA^+ movement were passive and if the volume of the cavity were constant throughout the duration of observation, as in the currently accepted model, the influx process would be linear with constant coefficients. This prediction can be tested by analyzing the system's response to a forcing function. The forcing function used in these studies is a step in which luminal $[TMA^+]$ goes from 0 to 10 mmol l^{-1} at time zero. When the data include both influx and efflux, the forcing function consists of a step wherein luminal $[TMA^+]$ goes from 0 to 10 mmol l^{-1} at time zero and then back to 0 mmol l^{-1} when efflux starts.

A first-order linear system with constant coefficients would respond exponentially to a step input. The response could be analyzed with semi-logarithmic plots. However, if the response were of higher order, it would be difficult to extract much information from a semi-logarithmic plot without an *a priori* model. An alternative is to carry out analysis in the phase plane (Grimshaw, 1990). The phase plane diagram, a plot of $df(t)/dt$ as a function of $f(t)$, shows whether a given system behaves as a first-order system or, if it does not, suggests the nature of the higher-order system.

In the phase plane, values of f obtained during influx plot above the x-axis (positive derivative) and those obtained during efflux plot below the x-axis (negative derivative). Time increases as one moves to the right for values for which $df/dt>0$, and to the left for values for which $df/dt<0$. The response to a step function of a first-order linear system with constant coefficients plots as a straight line during influx. The intercept on the df/dt-axis is the initial influx rate and that on the f-axis is the equilibrium value of f. If efflux is also included, there is an instantaneous drop to the most negative value of df/dt and a subsequent straight line path going to the origin.

Predictions for a first-order system

The following are strict predictions for TMA^+ influx and efflux as they would appear in the phase plane if the system were first order, i.e. a direct passive path between gut lumen and goblet cavity. (1) Both the influx and efflux functions of $d[TMA^+]/dt$ would be linear functions of $[TMA^+]$. (2) The equilibrium value of influx is $10\times\exp$(goblet-to-lumen potential difference/25.43) if TMA^+ behaved as a free cation, or 10 if it did not; $[TMA^+]$ is 10 mmol l^{-1} in luminal solution. A corollary of these two predictions is that $d[TMA^+]/dt$ at any time is proportional to the difference between $[TMA^+]$ at that time and the equilibrium value. (3) At the end of exposure, $d[TMA^+]/dt$ is discontinuous and efflux starts immediately; maximum $[TMA^+]$ must occur at this time. The presence of a pre-compartment would cause the system to depart from this prediction. Some unstirred layer is expected in this preparation, so the prediction should be relaxed for the expectation that there will be a very rapid change in $d[TMA^+]/dt$, maximum $[TMA^+]$ must occur very shortly after the change from influx to efflux and the maximum value of $[TMA^+]$ can be only slightly above the value attained at the end of exposure. A related prediction in the time domain is (4) that the curve of $[TMA^+]$ as a function of time is always concave downwards during exposure and concave upwards during leach-out. If this prediction is modified to allow for the presence of an unstirred layer of reasonable size, the plot of TMA^+ as function of time should be initially concave upwards. For an unstirred layer of 65 μm, estimated in Moffett *et al.* (1995), the inflection point should occur in less than 5 s. In the same way, the curve for efflux is initially concave downwards, but the inflection point for efflux should occur within 5 s.

Fig. 1 shows the phase plane diagram expected for a terminated step function applied to the single-compartment system. In this example, the slopes of the lines obtained from influx and efflux are the same, but that is not a requirement. If there were a voltage difference between the source and the single compartment or if there were convective flow, the slopes would differ, but each would still be a straight line.

Predictions for second-order systems

The curvature seen in the phase plane for step functions applied to two-compartment systems is equivalent to the statement that the forcing function does not appear as a step function in the compartment being monitored. The direction of

the curvature is diagnostic of the order of compartments. If the second compartment is in front of the one being monitored (pre-compartment), the influx curve will be convex upwards and the efflux curve convex downwards (Fig. 2A,B). If the second compartment is behind the one being monitored (post-compartment), the influx curve will be concave upwards and the efflux curve concave downwards (Fig. 2C,D). If the second compartment equilibrates rapidly, the transition to first-order behavior in each curve would be early in time; i.e. at low values of *f* during influx and high values during efflux (Fig. 2A,C). If the second compartment equilibrates slowly, the transition to first-order behavior in each curve will be late in time; i.e. at high values of *f* during influx and low values during efflux (Fig. 2B,D).

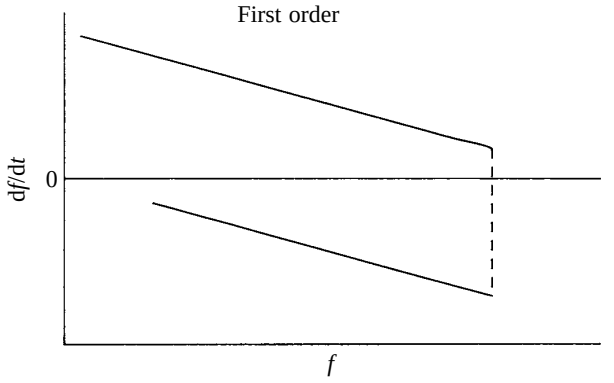

Fig. 1. Path in the phase plane diagram of a first-order linear differential equation with constant coefficients in response to a terminated step input. The upper curve is generated during exposure, and time increases as one moves to the right. The lower curve is generated during leach-out and time increases as one moves to the left. At the termination of exposure, d*f*/d*t* changes discontinuously from positive to negative.

The slopes of the lines when the system is showing only first-order behavior give the rate constants for influx and efflux. The rate constant of a compartment is approximately the ratio of the rate of transfer of TMA^+ into the compartment to the quantity of TMA^+ present at equilibrium ($[TMA^+]_{eq}$). Thus, a low rate constant is a reflection of a low TMA^+ transfer rate, a large compartment volume or a high $[TMA^+]_{eq}$. Indeed, as illustrated in Fig. 2D, if there is a very slow post-compartment, the change in slope may not appear during efflux and the plot may appear to be going to a non-zero intercept. Finally, $[TMA^+]_{eq}$ can be estimated by regression to zero time of influx points obtained during the period dominated by the first-order process. Regression of points obtained from efflux should have $[TMA^+]_{eq}=0$.

Results

Goblet cavity kinetics under short-circuit conditions

Forty-seven acceptable impalements were made under short-circuit conditions (SC). Fifteen of these showed TMA^+ influx rates greater than $10\,\mu mol\,l^{-1}\,min^{-1}$. Of these, 10 yielded sufficient data for complete analysis. Six of these had data for both influx and efflux. All but one showed a pre-compartment. In the majority of cases, the pre-compartment was quite obvious and influx was clearly concave upwards initially (Fig. 3). However, in one case (Fig. 4), the pre-compartment was virtually undetectable.

A pre-compartment as rapidly equilibrating as indicated by the data shown in Fig. 4 could have been an artifact of data filtering in combination with a small unstirred layer on the luminal side. Nevertheless, the data shown in Fig. 4 are still inconsistent with direct entry of TMA^+ into the goblet cavity. In this impalement, V_{gl} (the potential difference between the goblet cavity and the luminal solution) was +35 mV. With V_{gl}=35 mV and 10 mmol l^{-1} TMA^+ in the luminal solution, the

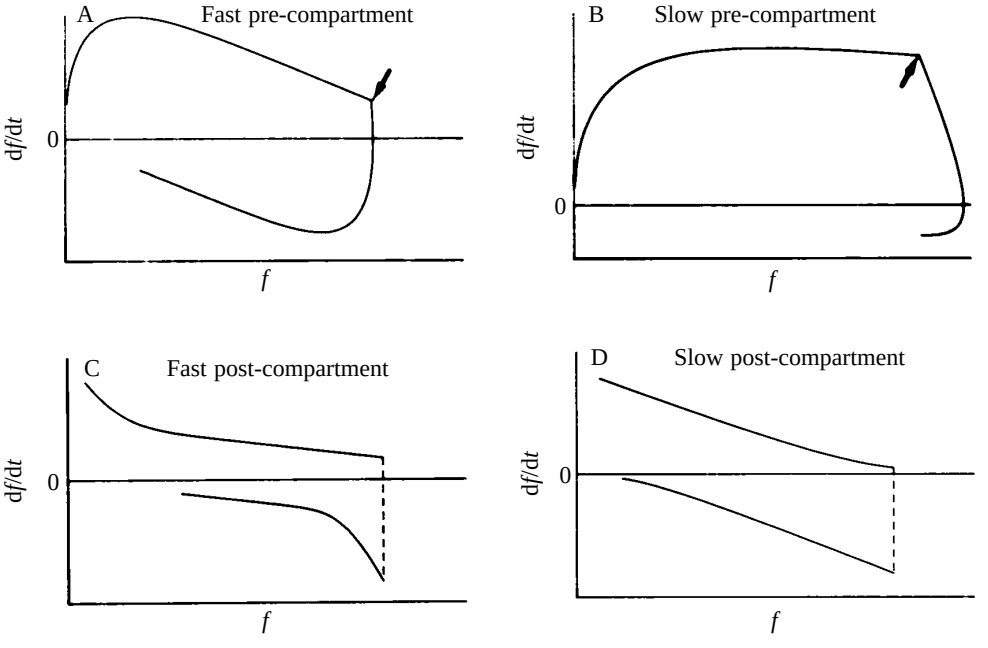

Fig. 2. Phase plane diagrams for a two-compartment system. The behavior of the system in response to a step-forcing function with a fast and slow pre-compartment and with a fast and slow post-compartment is shown in A–D. In A and B, the change from uptake to washout is indicated by an arrow. In C and D, the change is instantaneous and is indicated by a dashed line.

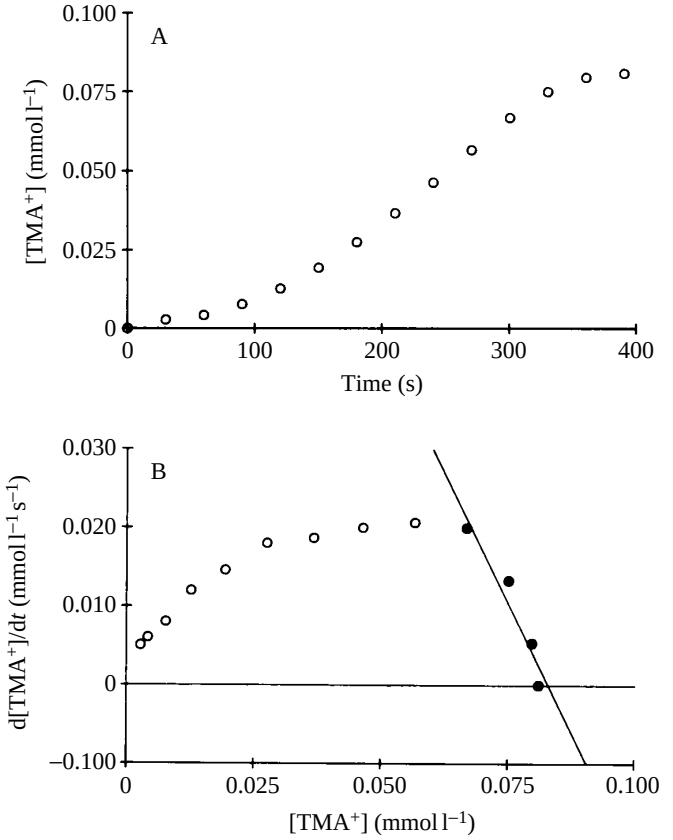

Fig. 3. (A) Time course of influx of TMA^+ in a typical short-circuited preparation. Successive points have been filtered with a moving average window of three. (B) Phase plane diagram of this experiment. In this and subsequent phase plots, the filled symbols are those upon which a regression has been performed; dt=30 s.

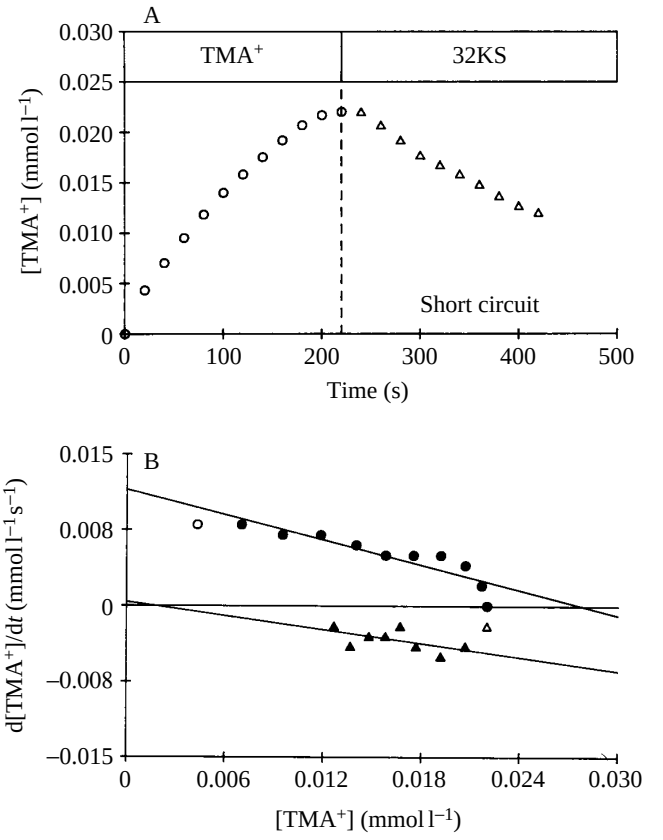

Fig. 4. (A) Time course of influx of TMA^+ into a tissue with an unusually fast pre-compartment under short-circuit (SC) conditions. Successive points have been filtered with a moving average window of three. Note that the influx curve is convex upwards. In this and subsequent figures, values obtained during exposure are plotted as circles and those obtained during leach-out are plotted as triangles. (B) Phase plane diagram of this experiment. The regression line for efflux is determined from the filled triangles; dt=40 s.

$[TMA^+]_{eq}$ in the goblet cavity predicted by the Nernst equation is 2.5 mmol l^{-1}, whereas regression of the influx data in the phase plane diagram predicts $[TMA^+]_{eq}$=0.028 mmol l^{-1}. If there is a pre-compartment, the early points must be eliminated from the regression, for those reflect the way the forcing function seen by the goblet cavity differs from a step function. This regression was performed on all but the first point. If all points are included, the predicted value is 0.029 mmol l^{-1}. Deletion of the first two points leads to a prediction of 0.027 mmol l^{-1}.

In only four experiments did TMA^+ influx slow sufficiently to allow a meaningful regression of the phase plot. In each case, the equilibrium concentration of TMA^+ as computed from regression in the phase plane was much lower than predicted by the Nernst equation, ranging from a factor of 100 in the experiment depicted in Fig. 4 to a factor of 9 in the experiment depicted in Fig. 10A.

Goblet cavity kinetics under open-circuit conditions

Sixty-eight acceptable penetrations were made under open-circuit conditions (OC). Twenty-one of these showed TMA^+ influx rates greater than 10 μmol l^{-1} min^{-1}. Of these, 10 yielded sufficient data for complete analysis. Seven of these had data for both influx and efflux. All but one showed a pre-compartment. A typical result (Fig. 5) shows the long concave-upwards curve during influx that is diagnostic of a pre-compartment. A second indication of a pre-compartment in the open-circuit condition is the observation that $[TMA^+]_g$ continued to rise after the TMA^+ had been removed from the superfusate. This overshoot of $[TMA^+]_g$ was observed in all impalements of normal OC preparations in which any TMA^+ entered the goblet cavity. A final characteristic of the OC preparations was that $[TMA^+]_g$ was higher in the OC than in the SC preparations late in the exposure.

In only two of the 10 OC experiments analyzed did TMA^+ influx slow sufficiently to allow a meaningful regression of the phase plot. In both of these, the equilibrium concentration of TMA^+, as determined by regression, was less than one-tenth of that predicted from the Nernst equation.

Two additional impalements under OC from a single tissue in which transepithelial potential (V_{oc}) was less than 20 mV (although V_g, the transepithelial potential of the goblet cell,

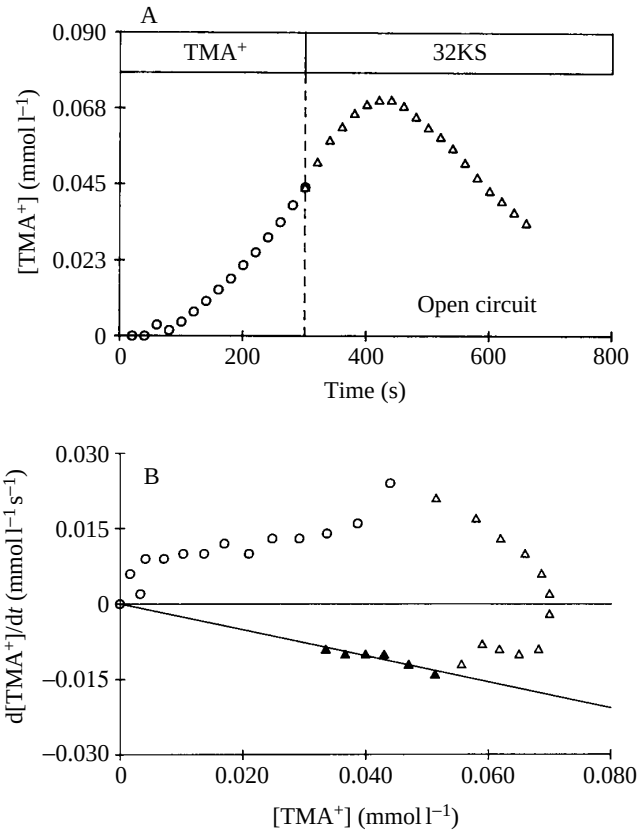

Fig. 5. (A) Time course of influx of TMA^+ in a typical open-circuit (OC) preparation. Successive points have been filtered with a moving average window of three. (B) Phase plane diagram of this experiment. See Figs 3 and 4 for an explanation of the symbols; dt=20 s.

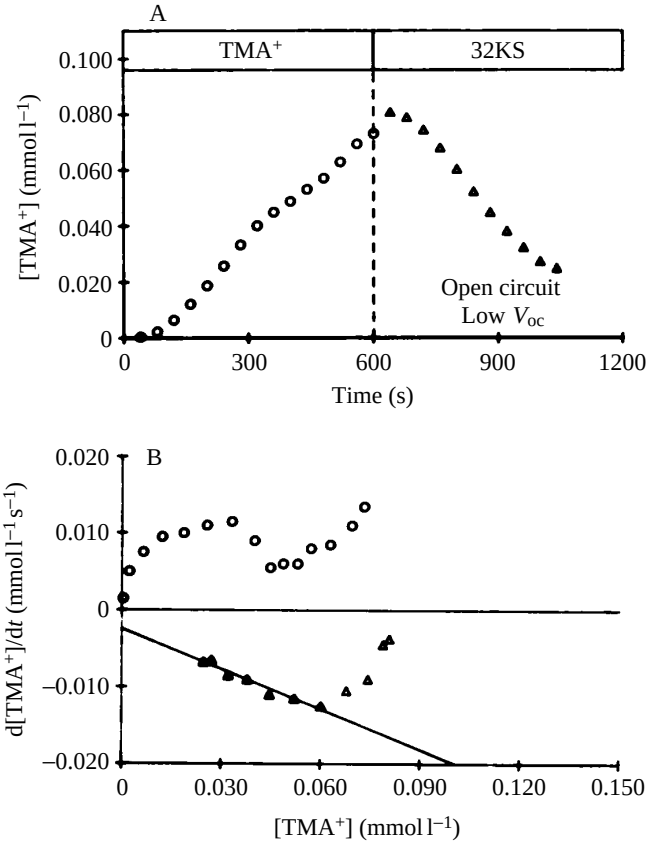

Fig. 6. (A) Time course of influx of TMA^+ in an OC preparation with a very low V_{oc}. However, both V_g and intracellular K^+ activity were high in the goblet cavity, so these cells were healthy. Successive points have been filtered with a moving average window of three. (B) Phase plane diagram of this experiment. See Figs 3 and 4 for an explanation of the symbols; dt=40 s.

was high) were analyzed. These were apparently healthy goblet cells in a tissue that, for some reason, did not generate a high V_{oc}. The special condition of these healthy cells in a tissue with low V_{oc} answers some possible questions. In the result shown in Fig. 6, V_{oc} was 6 mV, but V_{gl} was +57 mV. Thus, the electrical conditions were much like those of normal SC conditions. The plot shows little concavity during influx and little overshoot, indicating a fast pre-compartment, like that of an SC preparation. These results suggest that the presence of a slow pre-compartment depends on a high value of V_{oc} rather than on the presence or absence of a current passing through that particular cell.

Cytoplasm

Of ten impalements identified as cytoplasmic by the criteria of Moffett and Koch (1988*a*), four showed entry of TMA^+. Two of these allowed complete analysis of both influx and efflux. Fig. 7 shows the results of one of these. There was a rapid pre-compartment and very little overshoot. In these respects, the data resemble goblet cavity data from SC preparations. The one impalement that was followed for a long time showed a definite post-compartment. This finding of a post-compartment during efflux was never seen in normal goblet cavity impalements.

Effects of cytochalasin

As shown by Moffett *et al.* (1995), cytochalasin E dramatically enhances TMA^+ entry into goblet cavities, but only into those already accessible to TMA^+. Peculiar features of these results are: (1) SC preparations showed a very large overshoot, a phenomenon which was otherwise seen only under OC conditions, and (2) both OC and SC preparations showed a distinct post-compartment. These features are reflected in the phase plane plot of a typical experiment (Fig. 8) which shows a concave downwards influx curve and an efflux curve that regresses to a positive value of $d[TMA^+]/dt$. In addition, it should be noted that both the influx and efflux rates reach much higher values than in the normal experiments. These results suggest that cytochalasin E greatly enhanced both the path from a pre-compartment into the goblet cavity during influx and the reverse pathway during efflux, and also that $[TMA^+]_{eq}$ in the pre-compartment is higher than luminal $[TMA^+]$.

Model

As discussed by Moffett *et al.* (1995), the obvious conclusion from these studies is that there is no entry of TMA^+

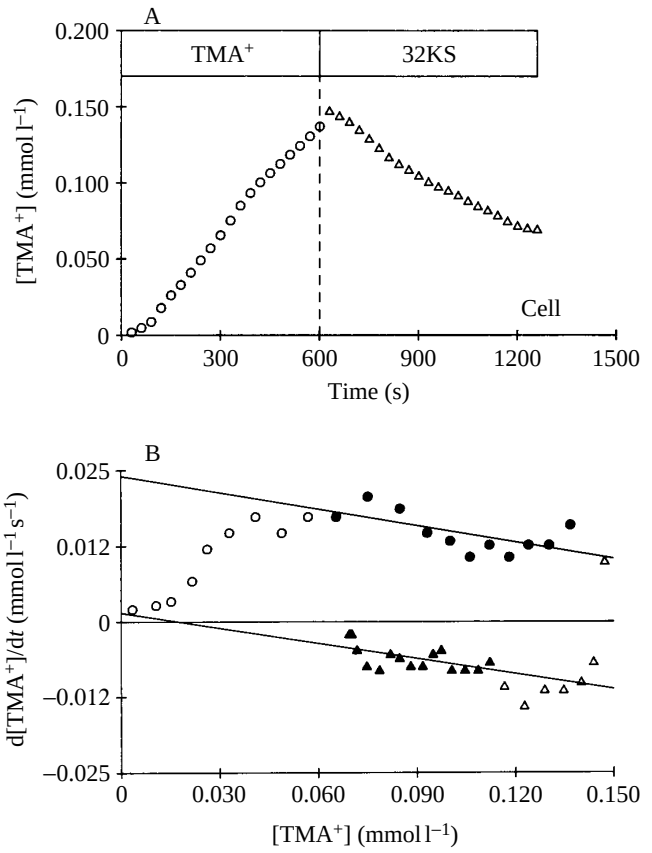

Fig. 7. (A) Time course of influx of TMA^+ into a cell in an SC preparation. Successive points have been filtered with a moving average window of three. (B) Phase plane diagram of this experiment. Note that efflux does not approach zero, providing evidence for a post-compartment. See Figs 3 and 4 for an explanation of the symbols; dt=30 s.

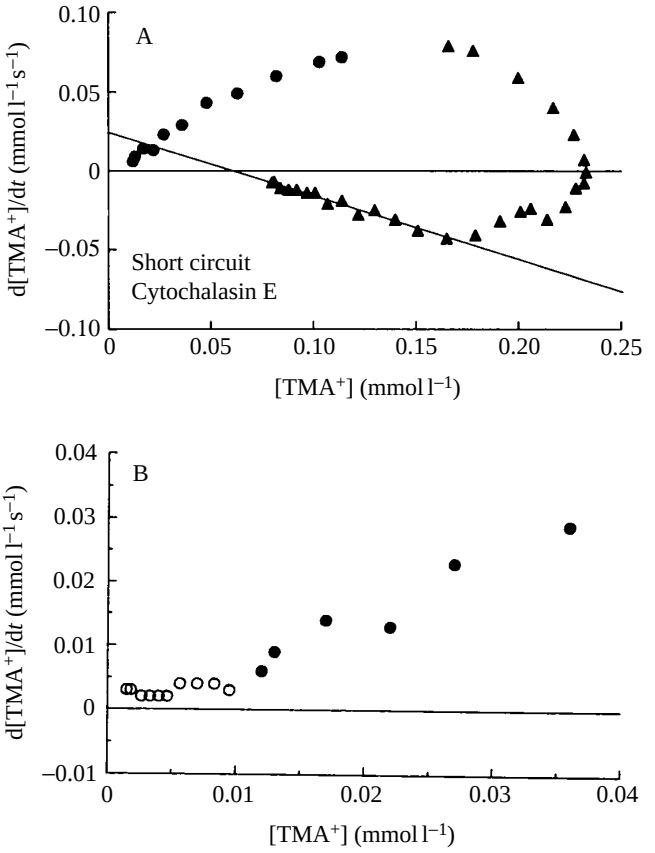

Fig. 8. (A) Phase plane diagram of TMA^+ influx and efflux under short-circuit conditions after treatment with 10^{-5} mol l^{-1} cytochalasin E. Symbols as in Figs 3 and 4; dt=20 s. (B) The first 340 s of the experiment, showing TMA^+ influx points before cytochalasin treatment (open circles) and the first 120 s after treatment (filled circles).

from the gut lumen through the goblet cavity valve. The present analysis shows that in those goblet cavities that did experience TMA^+ entry there was at least one intervening compartment between the gut lumen and the goblet cavity. Evidence presented earlier (Moffett *et al.* 1995) enabled us to rule out a luminal unstirred layer as an artifactual pre-compartment. In the one cell impalement that had a long efflux, there was clear indication of a compartment present after the cell. Finally, the estimates of $[TMA^+]_{eq}$ obtained from regression of the data when plotted in the phase plane are much too low to be explained by a Nernstian equilibrium distribution of TMA^+ between the lumen and the cavity. These results preclude a first-order system and compel us to consider TMA^+ entry routes for goblet cavities that include a pre-compartment. All such models require TMA^+ to cross cell membranes. In designing the present studies, we had assumed TMA^+ to be impermeant, on the basis of its use as a marker for the measurement of cell volume (Cotton and Reuss, 1991). However, we found that TMA^+ entered the cytoplasm in four of eight impalements. This unexpected result cannot readily be explained as an artifact of impalement damage, since the TMA^+ is applied to the luminal surface and the impalements are through the hemolymph surface.

In all models constructed, the compartments were well-stirred and there was no diffusion over distance. Transfer between compartments was passive and proportional either to the difference in concentration or to the electrochemical potential. Logically, any such model must contain at least two pre-compartments and therefore must be at least a three-compartment model. Goblet cell cytoplasm would be the second compartment and would feed into the goblet cavity. There must be another pre-compartment that feeds into the goblet cavity. This might be the lateral interstitial space (LIS) or the cytoplasm of a columnar cell. However, if either of the pre-compartments is kinetically fast, the system might be adequately described with only one pre-compartment and modeled as a two-compartment system.

To be considered successful, a model had to simulate the experimental data for a panel of test experiments selected to have both influx and efflux and to be as diverse in values of short-circuit current (I_{sc}) or open-circuit transepithelial potential (V_{oc}) as possible. In addition to a general match of

the data points, three other criteria were used to judge the fit of the model to each experiment. The first was that the computed results had to show the correct dominant curvature during influx. Almost all of the experimental data showed an initial concave upwards portion to the influx. However, the inflection point was early for some SC preparations and the dominant curvature was convex. For other SC preparations, the inflection point came late and influx was generally concave. For the OC preparations, the inflection point generally came late and influx was concave upwards for most or all of its duration. The second criterion was that the magnitude of the overshoot, that is, the amount by which $[TMA^+]_g$ rose after luminal TMA^+ had been returned to zero, had to be matched by the model. Finally, the time after the change-over from influx to efflux at which the overshoot reached its peak value had to match between model and data.

Several two-compartment models were tried, including those in which the first compartment was LIS (and goblet cell cytoplasm was assumed to equilibrate rapidly either with LIS or goblet cavity), and those in which the first compartment was a columnar cell (and both LIS and goblet cell cytoplasm equilibrated rapidly). None of these models proved able to match the rate of TMA^+ rise during influx and fall during efflux, nor could they produce the overshoot that is a prominent feature of the OC data.

Accordingly, two three-compartment models were tried. In the first, LIS was the first pre-compartment and the goblet cell cytoplasm was the second. In the second model, the columnar cell cytoplasm was the first pre-compartment and the goblet cell cytoplasm was the second. These models differ in the volumes of the compartments and in the way that voltage enters into the relationships.

Preliminary investigation of the solutions showed that the first compartment required a volume of at least $0.1\,ml\,g^{-1}$ tissue to fit the observed curvatures during influx and the observed overshoots. Better fits were obtained when the volume of the first compartment was at least $0.25\,ml\,g^{-1}$ tissue. These findings appear to eliminate LIS as the first pre-compartment and require that TMA^+ cross the apical membrane of columnar cells. Columnar cells of the midgut engage in endocytosis, as indicated by the finding that, after a ferritin meal, they contained large amounts of ferritin, although none appeared in the goblet cavities (Smith *et al.* 1969). We suggest that TMA^+ enters the columnar cell by this mechanism.

The model requires communication between columnar cell and goblet cell cytoplasm. This might occur *via* gap junctions or it might involve a small and kinetically invisible LIS. Unfortunately, evidence for cell–cell coupling in this tissue is not unanimous. An early study (Blankemeyer and Harvey, 1978) did not detect electrical coupling under the conditions used in the present study. However, in that study goblet and columnar cell impalements were identified on the basis of an inferred difference in potential difference across the basal membrane (V_b) between the two types, rather than by a positive identification of the particular cells impaled. In particular, goblet cells were inferred to have a V_b of only a few millivolts. The suppositions that 'low-potential cells' were goblet cells, or that valid penetrations of either cell type had been made, were refuted by studies (Moffett *et al.* 1982; Thomas and May, 1984) in which individual impaled cells were dye-marked and positively identified by subsequent microscopy.

Several studies (Moffett *et al.* 1982; Thomas and May, 1984; Baldwin *et al.* 1993) have used cell-to-cell movement of ionophoresed fluorescent dye ('dye coupling') as an indicator of intercellular coupling. In fifth-instar animals, such as those used in these studies, we found some columnar cells to be 'dye-coupled' to adjacent goblet cells (Moffett *et al.* 1982), although such coupling was not seen by other workers, at least in earlier instars (Thomas and May, 1984; Baldwin *et al.* 1993). However, as demonstrated by Blennerhassett and Caveney (1984) for insect integumentary cells, coupling for small inorganic ions may exist in the absence of dye coupling. Perhaps the best evidence for goblet cell/columnar cell coupling for K^+ (as contrasted with dye) is the finding (Moffett and Koch, 1988*a*) that no systematic difference can be resolved between the transapical potentials or intracellular K^+ activities of the two cell types.

In any case, the finding that only about half of the goblet cavities are accessible to TMA^+ is consistent with our earlier dye ionophoresis studies (Moffett *et al.* 1982), which showed that a similar fraction of goblet cells were dye-coupled to one or more adjacent columnar cells. Assuming that there is limited coupling between goblet and columnar cells, the reason TMA^+ failed to enter some goblet cavities may be that, at that moment, those goblet cells were not coupled to columnar cells.

The high influx rate and overshoot seen in the experiments with cytochalasin E suggest enhanced transfer between a pre-compartment and the goblet cavity. In these experiments, the early kinetics are not very useful for analysis because we do not know the time course of cytochalasin entry. The projection of late efflux to a positive value suggests that cytochalasin also enhances TMA^+ movement from the goblet cavity to a post-compartment within the tissue. Both of these results are consistent with enhanced cell–cell coupling, with the columnar cells acting as the other compartment. Furthermore, if cytochalasin and cyclic AMP enhanced the rate of entry of TMA^+ into columnar cells, they would be effective for coupled goblet cells but not for uncoupled cells, which is consistent with the observed association between some initial TMA^+ uptake and subsequent stimulation of uptake by cytochalasin and cyclic AMP.

The model also requires transfer of TMA^+ from the goblet cell cytoplasm to the goblet cell lumen. Under suitable conditions, Na^+, Li^+ and NH_4^+ can all be transported by the midgut (Zerahn, 1971), although at lower rates than for K^+ and Rb^+. According to the present view, this means that they can be accepted by the K^+/nH^+ antiporter (Wieczorek *et al.* 1991). It seems reasonable to expect the antiporter to accept TMA^+, albeit perhaps at a reduced rate.

The three-compartment model rationalized above is shown in Fig. 9. The equations for this model during exposure are:

$$C_x dX/dt = G_1(10p - X) - G_2(X - Y) - G_3 X p_p, \quad (1)$$

$$C_y dY/dt = G_2(X - Y) - G_4(Y - Zq) - G_5 Y p_p, \quad (2)$$

$$C_z dZ/dt = G_4(Y - Zq), \quad (3)$$

where X, Y and Z are the concentrations in the columnar cell, the goblet cell cytoplasm and the goblet cavity, respectively, C_x, C_y and C_z are the volumes of these compartments, p, p_p and q are voltage weighting terms and 10 is luminal [TMA^+] (in mmol l^{-1}). G_1–G_5 are rate constants for transfer across the boundaries of the compartments. p = exp(luminal voltage minus cellular voltage), p_p = exp(cellular voltage) and q = exp(goblet cavity voltage minus cellular voltage), where the voltages are expressed in multiples of $F/\boldsymbol{R}T$ and with respect to the basal surface. The forcing function for the system is the term '10p' in equation 1. This term is zero for efflux.

This model describes the [TMA^+] in three compartments, only one of which is sampled. Normally, Z for the goblet cavity is measured, although we also have measurements of Y for the goblet cell cytoplasm. It requires a total of 11 parameters to define the model: the three volumes, the three voltages and the five rate constants. Two of these are measured, transepithelial potential and the voltage in the compartment monitored. This leaves nine free parameters in the system. As discussed below, we were able to reduce the number of free parameters to five.

Reduction of free parameters

Morphometric measurements of light micrographs of midgut tissue suggested volumes of approximately 0.35 ml g^{-1} tissue for columnar cell cytoplasm, 0.1 ml g^{-1} for goblet cell cytoplasm and 0.30 ml g^{-1} for goblet cavity. The sum of these then makes up the total fluid volume of the tissue of approximately 0.75 ml g^{-1} tissue (Koch and Moffett, 1987). Although the numerical values of the transfer coefficients were affected by the choice of compartment volumes, the model was able to yield a satisfactory fit for each experiment so long as compartmental volumes were near those values.

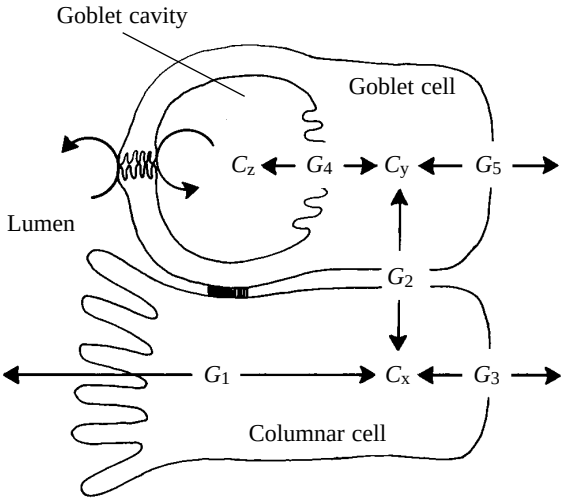

Fig. 9. Three-compartment model used to fit the data. The symbols are explained in the text. The curved arrows indicate that TMA^+ cannot cross the valve but is reflected.

When the impalement was in a goblet cavity, the unmeasured voltage was the cellular voltage (V_b). This was required to be between −25 and −55 mV for SC and between −15 and −40 mV for OC. These values correspond to those measured in

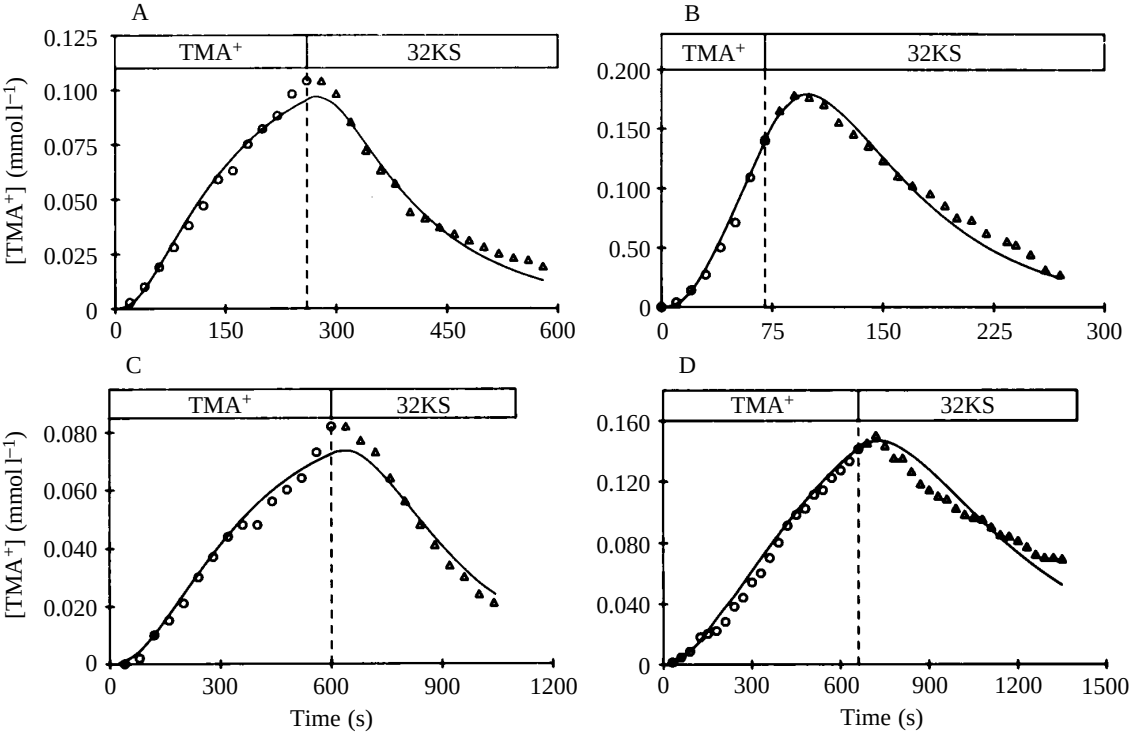

Fig. 10. Examples of comparisons of the data with the model. The experimental points depicted here are unfiltered. (A) SC; (b) OC; (C) OC in low-V_{oc} tissue (same experiment as shown in Fig. 6); (D) cell (same experiment as shown in Fig. 7). The circles are for exposure and the triangles are for leach-out, and the line gives the values for the model.

Table 1. *Values for the parameters from the model*[1]

	G_1 (s^{-1})	G_2 (s^{-1})	G_3 (s^{-1})	G_4 (s^{-1})	G_5 (s^{-1})
SC	0.210±0.033	2.43±0.61	4.14±0.83	6.26±4.17	6.29±0.94
OC	0.282±0.079	3.73±0.95	5.08±1.68	0.029±0.12	5.75±2.03
low-V_{oc} OC	0.230	3.00	4.5	0.06	3.00
Cell	0.013±0.002	1.8±1.6	7.00±1.73	–[2]	4.83±1.88
Average	0.241[3]	2.82[4]	4.97[4]	0.037[5]	5.50[4]

N for SC = 7, OC = 4, low-V_{oc} OC = 2 and cell = 3.

The same volumes were used throughout. They were 0.35 ml g^{-1} tissue for columnar cell cytoplasm, 0.1 ml g^{-1} for goblet cell cytoplasm and 0.30 ml g^{-1} for goblet cavity.

[1]All values to be multiplied by 10^{-3}; [2]any value allowed a fit; [3]average of all 13 goblet impalements; [4]average of all 16 impalements; [5]average of the six OC impalements.

Values are means ± S.E.M.

our laboratory (Moffett and Koch, 1988*a*,*b*). After these limits have been placed on the unmeasured voltage and compartment volumes, only the five rate constants remain free. This system is sufficiently constrained to allow testing of the model.

Parameter estimation

It was not possible to optimize the parameters rigorously. The dominant curvature during influx, the location of the inflection points during both influx and efflux, and the presence and magnitude of overshoot are important features to match and they put strict limitations on the values of the parameters. These requirements are not readily amenable to computation. The matching process was therefore done by trial and error. Fig. 10 shows the fits for four different cases: SC, OC, OC with low V_{oc} and cell. The solutions are well-behaved and small changes in any parameter lead to only small changes in the computed solutions. The effects on the solution of variation in each parameter are monotonic. The parameter values are also robust. That is, one arrives at nearly the same values after starting from a variety of initial guesses. Thus, we consider these values to be close to the best estimates for the parameters.

Parameters were estimated for 13 goblet impalements in three groups (seven SC, four OC, two low-V_{oc} OC) and three cellular impalements (all SC). Transepithelial potential averaged 100.5 mV in the OC preparations, 13 mV in the low-V_{oc} OC ones and, of course, 0 mV in the SC preparations. Goblet-to-lumen potential averaged 36.3 mV in the SC, 10.8 mV in the OC and 56.5 mV in the low-V_{oc} OC group. Thus, very different driving forces were present in the different groups.

Generally, the values found did not depend on the experimental conditions. The values for G_2, G_3 and G_5 did not differ between groups. The values of G_1 were quite similar for all goblet impalements. However, G_1 was much lower in the three cellular impalements. The values for G_4, the rate constant for transfer into the goblet cavity, did differ markedly between SC and OC preparations. The average value of G_4 for all six of the OC preparations was about 0.5 % of the average for the SC preparations. Table 1 shows the average values for each of the parameters for each of the four groups as well as overall averages for those values that can be appropriately pooled.

Table 2. *Values of [TMA^+] in the three-model compartments as measured (experimental), as predicted by the model for the corresponding time (Mod-end) and as predicted by the model for the steady state (Mod-eq)*

	Columnar cell	Goblet cell	Goblet cavity
SC			
Experimental			0.080±0.016
Mod-end	2.36±0.51	1.13±0.275	0.076±0.015
Mod-eq	3.03±0.68	1.49±0.280	0.110±0.016
OC			
Experimental			0.289±0.170
Mod-end	187±84	132±68	0.279±0.157
Mod-eq	241±84	176±91	0.590±0.30
Low V_{oc}			
Experimental			0.081
Mod-end	4.76	3.58	0.064
Mod-eq	5.37	4.41	0.081
Cell			
Experimental		0.128±0.007	
Mod-end	0.436±0.13	0.135±0.005	0.003±0.0006
Mod-eq	0.572±0.16	0.221±0.005	0.005±0.0008

[TMA^+] is measured in mmol l^{-1}.

Values are means ± S.E.M.; *N*=7 for SC; *N*=4 for OC; *N*=2 for low-V_{oc} OC; *N*=3 for cell.

Table 2 compares the average values obtained experimentally with those predicted by the model for corresponding times. It also gives the steady-state concentrations of TMA^+ in each compartment, as computed by the model.

Discussion

The previous paper (Moffett *et al.* 1995) presented experimental evidence that TMA^+ could not cross the goblet cell valve. The significance of this finding is not so much in terms of TMA^+ as in terms of the way that K^+ enters the lumen. If K^+ passes directly from the goblet cavity into the gut lumen, it must do so *via* an ion-selective pathway, probably of channel dimensions.

Nevertheless, TMA^+ did appear in the goblet cavity in some of the preparations. Part of the justification of the experimental results is an explanation of how TMA^+ appeared in this cavity if it did not cross the goblet valve. It is important to emphasize that the actual rates at which TMA^+ moved are extremely low. The rates computed in this work are between 100- and 1000-fold slower than those for K^+ in the same tissue. Thus, although we did find that TMA^+ entered the cells and the goblet cavity, the rates at which it entered were so low as to be consistent with its use as an estimator of cell volume (Cotton and Reuss, 1991) or as an impermeant cation (Wieczorek *et al.* 1991).

It is conceivable that TMA^+ did not actually traverse cell membranes. The model proposes entry of TMA^+ from the lumen into the columnar cells. This could be pinocytotic, as could the exit across the basal membranes. Movement from columnar to goblet cell may be best explained as passing through gap junctions. These could be located in the septate desmosomes that join the columnar and goblet cells (Maxwell, 1981). This explanation would account for the finding that the fraction of impalements that showed entry of TMA^+ was approximately the same as the fraction of goblet cells shown to be coupled to the surrounding columnar cells (Moffett *et al.* 1982).

Cytochalasin E greatly enhanced the rate of entry of TMA^+ into and exit of TMA^+ from the goblet cavity. The data are not suitable for a kinetic analysis of TMA^+ uptake after administration of cytochalasin E because we do not know the time course of arrival of cytochalasin E at its point of action. If cytochalasin E has to act intracellularly, then the change in concentration of cytochalasin E at that intracellular point depends not only on the step function of cytochalasin E in the luminal superfusate, but also on the rate of its cellular uptake. The latter would most certainly introduce higher-order behavior into the onset of the cytochalasin E effect. We can, however, make some deductions from the behavior of $[TMA^+]_g$ after the tissue had been re-exposed to 32KS (see Moffett *et al.* 1995). The experiment depicted in Fig. 9 of Moffett *et al.* (1995) and in Fig. 8 here shows that, once the cytochalasin E effect is established, uptake continues unabated for some time after the lumen is again bathed in 32KS. Had cytochalasin E opened the goblet cell valves, then a sudden decrease in the rate of TMA^+ uptake would have been observed as the TMA^+ leaked through. The failure to observe a first-order component in the efflux after cytochalasin E treatment leads us to believe that cytochalasin E acts either at the initial columnar cell uptake step (G_1) or at the intercellular communication step (G_2). Cytochalasin was unable to initiate TMA^+ uptake; it was only able to enhance a pre-existing pathway.

There are several features of the way the data fit the model that are of interest.

(1) The rate constants other than G_4 are the same in SC and OC preparations. The voltage driving TMA^+ into columnar cells (transpical voltage) during SC is simply V_b, about 31 mV in this series. In the normal OC series, this voltage difference is the sum of V_{oc} and V_b and had an average value of 134 mV. In the two low-V_{oc} OC impalements, the average of the sum was 43 mV. The effects of these voltages are given by the term 'p'. 134 mV is equivalent to a concentration ratio of 204, whereas 31 mV is equivalent to a concentration ratio of 3.4. Thus, the force driving TMA^+ into the columnar cell differed by a factor of 204/3.4=60 between OC and SC conditions. Nevertheless, all of the goblet impalements were matched by the same value of G_1. The differences in behavior observed between SC, OC and the low-V_{oc} OC were attributable either to the characteristic difference of G_4 or to the different responses of the same system when exposed to different experimental conditions.

(2) The one point at which the model failed was the very low values of G_1 required to fit the cellular impalements. These impalements were from three different tissues, and we believe the low values of G_1 are a characteristic of the tissue, rather than a sampling aberration. One explanation of this would be that there are additional compartments in front of the cellular compartment that we sampled. This would lead to a model with four or more compartments. We did not believe the data justified trying so complex a model.

(3) The voltage difference between different compartments was necessary to bring about a fit of the model to the experimental data in all cases. This rules out movement of TMA^+ by an obligatory neutral ion-exchange, in which voltage sensitivity would not be expected.

(4) The rate constants for TMA^+ entry into the goblet cavity from the goblet cell cytoplasm were quite different between OC and SC preparations. We conclude that G_4 is tied to the rate of active K^+ transport. This suggests that the voltage-sensitive K^+/nH^+ antiport believed to transport K^+ across the GCAM (Wieczorek *et al.* 1991) can also accept TMA^+. This is not surprising in view of the ability of the midgut to transport all alkali metal ions and NH_4^+ (Zerahn, 1971). We believe that this result corroborates the generally accepted view that K^+ is actively transported into the goblet cavity and that it subsequently travels from there into the lumen during SC. However, this implies that the goblet valve is a structure that allows movement of K^+ out, but not an opening that allows passage of TMA^+.

(5) The selectivity of the goblet valve cannot be a consequence of an osmotically driven convective flow through the valve. Although this would produce asymmetry between influx and efflux rates, it would not change the system from first order.

(6) The higher driving force for TMA^+ from the lumen into the columnar cells during OC (p=204 rather than 3.4) explains two of the odd features of the experimental data. This higher driving force leads to higher cellular concentrations of TMA^+ during OC than during SC. As a result, goblet cavity concentrations are higher in OC. Furthermore, when efflux begins, although the cellular concentrations start to fall immediately, they remain higher than those in the goblet cavity for a time. TMA^+ continues to enter the cavity from this large cellular pool, even though luminal $[TMA^+]$ is zero, and this

appears as the overshoot. In SC, by contrast, cellular concentrations are low and rapidly fall below a level that will drive additional TMA^+ into the goblet cavity.

(7) The basal leaks from the cells (G_3 and G_5) explain two other features of the experimental results. First, leakage of TMA^+ through these pathways leads to equilibrium values of cellular [TMA^+] much lower than those predicted from the transapical voltage by the Nernst equation. The concentrations attained in the goblet cavity are correspondingly lower. The presence of these leaks also explains why the fit of the cellular impalements did not depend on the value of G_4. Although the values of G_3, G_4 and G_5 are all similar during SC, the voltage step from cell to cavity is greater than that from cell to basal surface. The average difference during SC was 36 mV, which implies an almost fivefold difference in driving force. Thus, changes in G_4 would only affect about 20 % of the TMA^+ leaving the cells; the rest leaves through the basal leaks.

In summary, the model rationalizes the distribution of TMA^+ in terms of the architecture of the tissue. It is robust under three different conditions of transepithelial potential (SC, OC, OC with low V_{oc}). It is consistent with currently accepted transport activities of the GCAM and with the ability of the midgut to transport a variety of monovalent cations. It is not consistent with passage of secreted K^+ through the goblet cavity valve by free diffusion or bulk flow. The term 'valve' for this structure may be a misnomer; further study of its role in determining the selectivity of the transport system for K^+ over H^+ is clearly needed.

This work was supported by a grant from the NSF, DC 8811354.

References

BALDWIN, K. M., HAKIM, R. S. AND STANTON, G. B. (1993). Cell–cell communication correlates with pattern formation in molting *Manduca* midgut epithelium. *Devl Dynam.* **197**, 239–243.

BLANKEMEYER, J. T. AND HARVEY, W. R. (1978). Identification of the active cell in a potassium transporting epithelium. *J. exp. Biol.* **77**, 1–13.

BLENNERHASSETT, M. G. AND CAVENEY, S. (1984). Separation of developmental compartments by a cell type with reduced junctional permeability. *Nature* **309**, 361–364.

COTTON, C. U. AND REUSS, L. (1991). Effects of changes in mucosal solution Cl^- or K^+ concentration on cell water volume of *Necturus* gallbladder epithelium. *J. gen. Physiol.* **97**, 667–686.

DOW, J. A. T. (1986). Insect midgut function. *Adv. Insect Physiol.* **19**, 187–328.

GRIMSHAW, R. (1990). *Nonlinear Ordinary Differential Equations*. London: Blackwell.

HARVEY, W. R. (1992). Physiology of V-ATPases. *J. exp. Biol.* **172**, 1–17.

KOCH, A. R. AND MOFFETT, D. F. (1987). Kinetics of extracellular solute movement in the isolated midgut of tobacco hornworm (*Manduca sexta*). *J. exp. Biol.* **133**, 199–214.

MAXWELL, D. J. (1981). The presence of gap junctions in the septate desmosomes of the salivary apparatus of the cockroach, *Nauphoeta cintrea*. *J. exp. Biol.* **94**, 341–344.

MOFFETT, D. F., HUDSON, R. L., MOFFETT, S. B. AND RIDGWAY, R. L. (1982). Intracellular K^+ activities and cell membrane potentials in a K^+-transporting epithelium, the midgut of tobacco hornworm (*Manduca sexta*). *J. Membr. Biol.* **70**, 59–68.

MOFFETT, D. F. AND KOCH, A. R. (1988*a*). Electrophysiology of K^+ transport by midgut epithelium of lepidopteran insect larvae. II. The transbasal electrochemical gradient. *J. exp. Biol.* **135**, 25–38.

MOFFETT, D. F. AND KOCH, A. R. (1988*b*). Electrophysiology of K^+ transport by midgut epithelium of lepidopteran insect larvae. II. The transapical electrochemical gradients. *J. exp. Biol.* **135**, 39–49.

MOFFETT, D. F., KOCH, A. AND WOODS, R. (1995). Electrophysiology of K^+ transport by midgut epithelium of lepidopteran insect larvae. III. Goblet valve patency. *J. exp. Biol.* **198**, 2103–2113.

SMITH, D. S., COMPHER, K., JANNERS, M., LIPTON, C. AND WITTLE, L. W. (1969). Cellular organization and ferritin uptake in the mid-gut epithelium of a moth, *Ephestia kuhniella*. *J. Morph.* **127**, 41–72.

THOMAS, M. V. AND MAY, T. E. (1984). Active potassium ion transport across the caterpillar midgut. II. Intracellular microelectrode studies. *J. exp. Biol.* **108**, 293–304.

WIECZOREK, H., PUTZENLECHNER, M., ZEISKE, W. AND KLEIN, U. (1991). A vacuolar-type proton pump energizes K^+/H^+ antiport in an animal plasma membrane. *J. biol. Chem.* **266**, 15340–15347.

ZEISKE, W. (1992). Insect ion homeostasis. *J. exp. Biol.* **172**, 323–334.

ZERAHN, K. (1971). Active transport of the alkali metals by the isolated midgut of *Hyalophora cecropia*. *Phil. Trans. R. Soc. Lond. B* **262**, 315–321.